Differential studies and projectile charge effects in ionization of molecular nitrogen by positron and electron impact

O. G. de Lucio[1] and R. D. DuBois[2]

[1]*Instituto de Física, Universidad Nacional Autónoma de México, Apartado Postal 20-364, Mexico Distrito Federal, Mexico*

[2]*Department of Physics, Missouri University of Science and Technology, Rolla, Missouri 65409, USA*

(Received 17 December 2015; revised manuscript received 29 February 2016; published 25 March 2016)

Singly, doubly, and triply differential information, obtained from coincidence measurements, are presented for 250-eV positron- and electron-impact ionization of molecular nitrogen. Comparisons of these data as functions of energy loss, scattering, and emission angles illustrate differences associated with the sign of the projectile charge. Via a deconvolution and normalization procedure, the triply differential data are converted to absolute cross sections. By fitting the triply differential cross sections for single ionization with simple functions, the intensities, directions, and peak to background intensities of the binary peaks plus the ratio of recoil to binary interactions are compared for positron and electron impact. Formulas for the binary and recoil intensities plus for the orientation of the binary peak as a function of momentum transfer are extracted from the data. Differences in the relative amount of fragmentation as a function of energy loss are also observed.

DOI: 10.1103/PhysRevA.93.032710

I. INTRODUCTION

Over the past decades ionization by electron impact has been exhaustively studied with special attention on describing inelastic interactions. Many of these studies have focused on measurements of ionization probabilities with the goal to fully describe the kinematics involved during and after the collision process. More recently, ionization by positron impact has been used to provide additional information that was unavailable, or not easy to extract, using only electron-impact data [1]. The main goals of such experiments are to provide accurate information on similarities or differences between particle-matter and antiparticle-matter interactions which aid in isolating certain processes and provide sensitive tests for theoretical models.

One particular interest in comparing positron- and electron-impact data are the differences in the interaction kinematics associated solely with the opposite projectile charges. These differences provide stringent tests of theory because first-order perturbation theories predict identical total and differential cross sections for higher-energy electron and positron impact whereas more sophisticated approximations developed in the 1980s and 1990s predicted differences in the differential electron emission measured as a function of the momentum transfer [2–13]. For example, in fully kinematic studies the binary electron emission (resulting from two-body interactions involving just the incoming projectile and a single target electron with the other bound electrons and target nucleus acting as nonparticipating spectators) was predicted to be enhanced (reduced) for positron (electron) impact; whereas just the opposite was predicted for the recoil intensity (corresponding to interactions where the ejected electron also interacts with the target nucleus as it leaves). The directions of the binary and recoil lobes were also predicted to have opposite shifts with respect to the momentum-transfer direction [5–9]. Many theoretical studies performed since then arrive at similar predictions [10–13].

On the experimental side, few differential comparisons between positron- and electron-impact data are available. This is because such measurements are difficult for positron impact due to the low signal intensities that are currently available. Until the late 1990s, the only data available for comparison purposes were the singly differential studies by Moxom *et al.* [14] and the doubly differential studies by Schmitt *et al.* [15] and by Kövér and co-workers [16,17].

However since then there has been systematic progress in overcoming the bottleneck of low beam intensities and in extending experimental differential studies to a wider range of kinematic conditions. Singly and doubly differential data are now available for double as well as single ionizations [18–21]. More importantly, the first triply (fully) differential studies were performed at University College London (UCL) in the 1990s [22–24] where scattered and ejected particles leaving in the extreme forward direction were measured in coincidence. These were followed by our work at the Missouri University of Science and Technology (MST) which covered a wider range of emission angles for the ionization of argon [10,21,25–30] plus in various conference presentations and papers. More recently, a collaborative effort between groups in Germany and Australia have reported triply differential data for positron-impact ionization of helium [31]. Limitations of the studies to date are that the UCL studies are restricted to 0° scattering and emission angles, the MST studies are only sensitive to small scattering angles, and low signal rates limit them to studying many electron targets, whereas for the German-Australian collaboration small cross sections restricted the amount of data obtained and analysis that could be performed.

Here we present the most comprehensive study to date where singly, doubly, and triply differential yields are measured and compared for 250-eV positron- and electron-impact ionizations of molecular nitrogen. These direct comparisons illustrate how a reversal of the direction of the Coulomb field between the projectile and the target leads to differences in the single-ionization yields and how these differences vary with scattering angle and energy loss, i.e., with momentum transfer. The triply differential data illustrate how reversing the direction of the field influences both the relative intensities and the directions of the binary lobe. In addition, relative differences in the fragmentation yields as a function of energy loss are shown.

II. EXPERIMENTAL METHOD

The experimental method has been described in detail previously [25,26]. In brief, a simple gas jet of molecular nitrogen is ionized by either a positron beam produced using a ^{22}Na source, a tungsten moderator, and an electrostatic transport system or by an electron beam originating from an electron gun inserted into the beamline. Thus, both beams enter the scattering chamber via the same input aperture and have the same trajectory, and data are collected using as identical conditions as possible which means that experimental uncertainties between the positron- and the electron-impact data are minimized. The beams intersect the target at the center of two biased plates used to produce a weak electric field (1.2 V/cm) perpendicular to the beam direction for the extraction of the target ions. The target ions are detected by a channeltron. These ions generate a stop pulse whereas scattered projectiles and ejected target electrons generate start pulses for two independent time-of-flight systems. Time-of-flight information establishes the target ion charge state and mass which distinguishes: (a) interactions leading to molecular ionization from those leading to fragmentation, (b) target versus background ionization, and (c) real versus random ionization events. Forward scattered projectiles, scattered by less than 5° in θ_p and between 0° ± 2.4° in φ_p are measured as a function of their scattering angle and energy loss by using an electrostatic energy analyzer and a position-sensitive channel plate. Here θ_p and φ_p represent angles in and perpendicular to the scattering plane. The detectable energy loss range is set by adjusting the spectrometer voltages. Electrons ejected from the target in geometric angles between 30° and 150° along and perpendicular to the beam direction are measured as a function of their detection angle using a second position-sensitive channel plate positioned above the interaction region and at 90° with respect to the beam direction. No energy analysis of the ejected electrons is performed by the apparatus. However, for single ionization their energies can be determined by using coincidences with projectiles that suffered a particular energy loss.

List mode data collection was used, thus allowing correlations among the various particles, angles, and energies to be established in order to obtain singly (SDCS), doubly (DDCS), and triply (TDCS) differential information about the ionization process as functions of scattering angle and energy loss. From this, differential information as functions of momentum transfer can be determined. Also, our method allows triply differential information to be generated for either the scattered projectile or the ejected electron.

III. RESULTS

A. Overview

Examples of DDCS data for 250-eV positron and electron impact on molecular nitrogen are shown in the upper left and right portions of Fig. 1 where the vertical axis is the projectile scattering angle in degrees (left axis) or in units of perpendicular momentum transfer (right axis), and the horizontal axis is the energy loss in eV (bottom axis) or in units of parallel momentum transfer (top axis). Here, the scattering geometry is such that negative scattering angles mean the projectile is

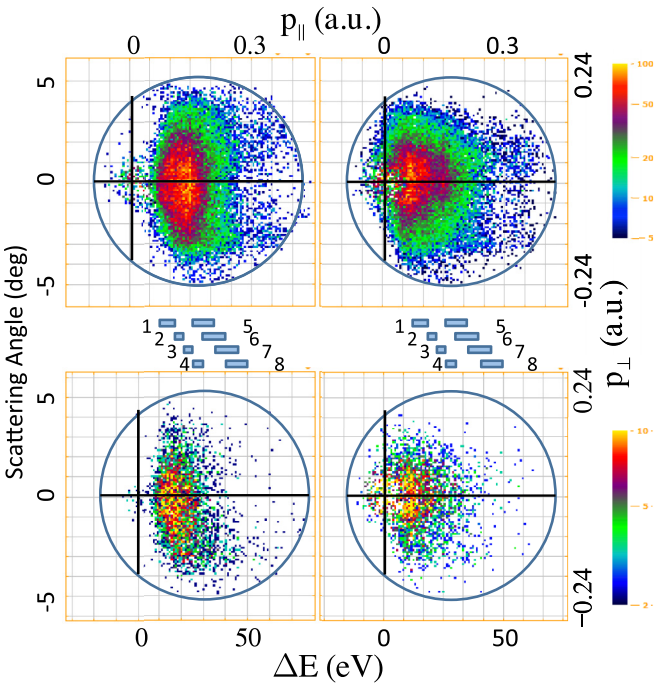

FIG. 1. DDCS (top) and TDCS (bottom) data for single ionization of molecular nitrogen by 250-eV positron (left) and electron (right) impact. The left vertical and bottom horizontal axes correspond to projectile scattering angle (degrees) and energy loss (eV). The top and right axes are the parallel and perpendicular momentum transfers in atomic units. The cross corresponds to the nonscattered beam position (0° scattering angle and 0-eV energy loss) with anomalies appearing at this point for electron impact being due to the subtraction of a relatively intense random signal. The boxes, labeled 1–8, shown between the upper and lower figures indicate energy loss ranges used when sorting the data, corresponding with: 17.5 ± 1.5, 19.6 ± 1.2, 22.8 ± 2.1, 28 ± 2.2, 31 ± 5, 35 ± 5, 41 ± 5, and 45 ± 5 eV.

scattered vertically downward whereas positive angles imply upward scattering. Since the electron detector is located above the interaction region, only upward emitted electrons are detected. Thus, the TDCS intensities for negative scattering angles, e.g., correlated downward scattered projectiles and upward emitted target electrons, are a direct indication of binary events since the scattered projectile and ejected electron are detected in "opposite directions." Likewise the intensities for positive scattering angles indicate recoil events because both particles are detected in the same hemisphere.

Although total cross-sectional measurements [32,33] show that electron impact is ∼25% less efficient than positron impact in the ionization of molecular nitrogen at this impact energy, to assist in making comparisons and to emphasize relative differences, our total ionization yields measured for positron and electron impact where the energy loss is less than ∼100 eV and the scattering angle is less than 5° have been normalized to each other. Thus, as seen in Fig. 1 using identical color scales for positron and electron impact, for single ionization of molecular nitrogen, 250-eV electrons scatter slightly less but lose more energy than positrons do. This holds, both for the doubly (top figures) and triply (bottom figures) differential data. Also, the triply (fully) kinematic

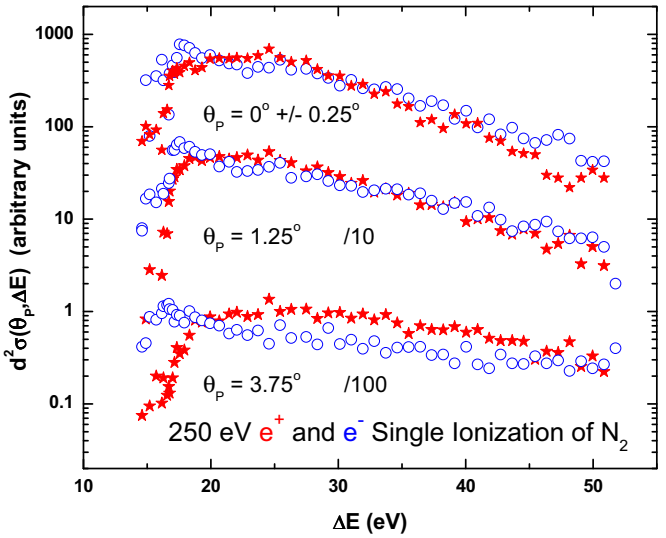

FIG. 2. DDCS data of the scattered projectile for different scattering angles θ_p as a function of the energy loss ΔE. The red stars correspond to positron impact, and the blue hollow circles correspond to electron impact. The 1.25° and 3.75° data have been divided by 10 and 100 for display purposes.

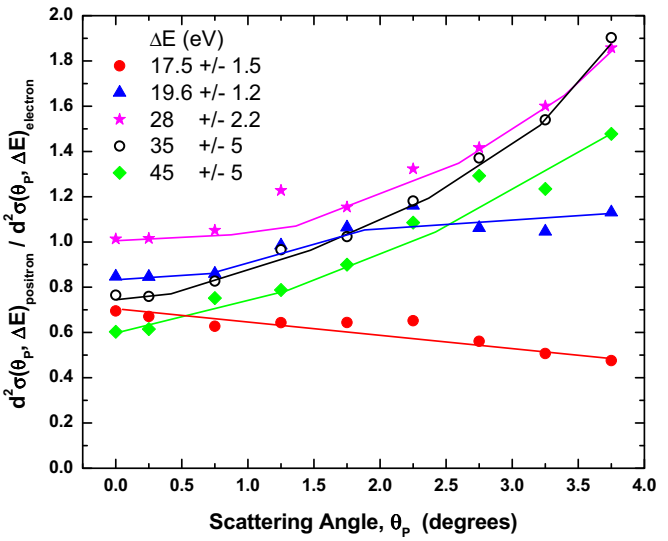

FIG. 3. Ratio of DDCS data of the scattered projectile for positron impact over corresponding data for electron impact as a function of the scattering angle θ_p for different energy losses ΔE.

electron-impact data have nearly identical probabilities for binary and recoil interactions whereas for positron impact there is a clear dominance in binary interactions, at least for kinematic conditions shown where the scattering angle is small.

B. Doubly differential comparisons: scattered projectile channel

For more detailed comparisons of the differences arising from positive and negative projectile charges, horizontal slices taken from the upper portion of Fig. 1, i.e., doubly differential energy loss information as a function of scattering angle, are shown in Fig. 2. The reader is reminded that here and in the following comparisons the electron-impact yields that are shown are approximately 25% too large due to our normalization. But this roughly corresponds to the size of the symbols used. Figure 2 shows that near threshold, 250-eV electrons have a larger probability of inducing ionization than positrons do, and this increased probability becomes larger with the scattering angle. Although our scattering angular range is limited, the trend of the data implies that the smaller total ionization cross section for electron impact arises from larger scattering angle interactions where the energy loss ΔE is greater than 20 eV. This is because $\sigma_{\rm tot} = \int d^2\sigma(\Delta E,\theta_p) \sin\ \theta_p d\theta_p d\ \Delta E$, where $\sigma_{\rm tot}$ is the total ionization cross section and $d^2\sigma(\Delta E,\theta_p)$ are the doubly differential cross sections shown in Fig. 2. Thus, when the ionization yields have similar magnitudes as in Fig. 2 the larger angle data are relatively more important because of the sin θ_p factor.

Figure 3 shows ratios of the positron- to electron-impact data for energy losses ranging from approximately 18 to 46 eV (energy loss bins 1–8 in Fig. 1). These ratios illustrate a dramatic increase with angle for larger energy losses, again revealing that interactions leading to higher-energy losses are more probable for positron impact than for electron impact. The solid lines serve only to guide the eye.

C. Singly differential comparisons: electron emission channel

Let us now consider the electron emission channel where information is provided by the ejected electron position-sensitive detector located above the interaction region. Using target electron-recoil ion coincidences, SDCS information proportional to $d\sigma(\theta)$ for electron emission as a function of observation angle is obtained. Ratios of the SDCS for positron to electron impact are shown in Fig. 4. These ratios show an enhanced emission for forward emitted electrons, i.e., for binary interactions, for positron impact, whereas electron

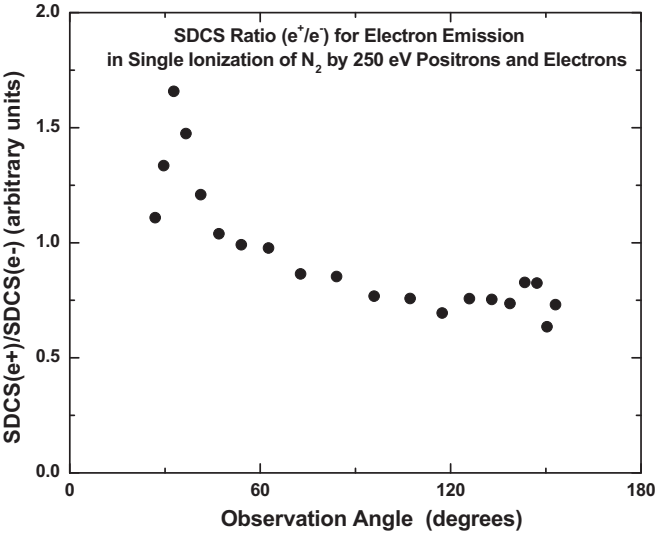

FIG. 4. Ratio of SDCS of electron emission for positron impact over corresponding data for electron impact as a function of the observation angle in the single ionization of N_2.

impact produces more emission in the backward direction, which arises from recoil interactions. Thus the ratios for forward and backward emission are greater than and less than 1, respectively. Our experimental method does not discriminate against scattered projectiles, which may partially contribute to the sharp rise and rapid decrease seen in the forward direction.

IV. TRIPLY DIFFERENTIAL CROSS-SECTIONAL COMPARISONS

The main aim of this paper was to measure and compare triply (fully) differential data for ionization of the nitrogen molecule by electron and positron impact as such data provide the most sensitive information about collision dynamics and for testing theoretical models. Triply differential information is obtained from recoil ion-scattered projectile-ejected electron coincidences. However, as our experiments are performed using beams considerably weaker than those traditionally used in fully differential studies, e.g., femtoamps rather than tens of nanoamps, our statistical uncertainties can be significant. In addition, our method employs an electric field to extract target ions and an extended, rather than a point, interaction region, both of which influence our detected electron emission.

Previously [27,28,30], to minimize statistical uncertainties we compared TDCS in the projectile scattering channel by comparing angular slices of the two-dimensional spectra shown in the bottom portion of Fig. 1. By comparing triply to doubly differential ratios as a function of scattering angle and energy loss, i.e., vertical slices taken from the lower and upper portions of Fig. 1, any artifacts associated with electric-field effects on the ejected electron trajectories as well as any contribution from solid angle effects are removed or considerably reduced since the influence of such parameters is the same for both the doubly and the triply differential data. This also removes any experimental asymmetries between positive and negative scattering angles since by definition the DDCS must be symmetric. We found that for positron impact the ratios are nearly isotropic for recoil events and showed a monotonic increase for binary events with the increase becoming larger with energy loss, i.e., with momentum transfer. Thus, the relative probability of binary to recoil interactions increases as a function of scattering angle, i.e., with perpendicular momentum transfer, and with energy loss, i.e., with total momentum transfer. The available data imply this to be independent of target species and impact energy [27]. For electron impact, the findings were similar, but the increases as functions of scattering angle and energy loss for binary interactions were weaker than those for positron impact.

With regard to the traditional method of comparing TDCS, meaning in the electron emission channel, in a previous study of ionization of argon [10] we compared our measurements with theoretical predictions by convoluting the theory over our experimental parameters. Doing so unfortunately obscures important features with respect to binary and recoil lobe intensities and directions. For the present study, the availability of data from Avaldi *et al.* [34] allows us to improve our convolution function which then allows us to normalize our measured triply differential yields and place them on an absolute scale.

This was performed in the following manner. The continuous distributions of TDCS data as functions of the projectile scattering angle and energy loss plus the ejected electron observation angle shown in the lower portion of Fig. 1 were binned with respect to scattering angle and energy loss and used to sort the ejected electron angular distributions. Doing so means that the total counts contained in each of these bins are divided among the entire electron emission angles we are sensitive to. As a result, especially for larger scattering angles and energy losses and particularly for the recoil lobe, the statistics are limited. To compensate for this, various combinations of data binning were used. As a compromise between available statistics and acceptable energy and angular resolution, three scattering angle bins of $1^\circ \pm 0.5^\circ, 2^\circ \pm 0.5^\circ$, and $3^\circ \pm 0.5^\circ$ and eight energy loss bins of $17.5 \pm 1.5, 19.6 \pm 1.2, 22.8 \pm 2.1$, 28 ± 2.2, 31 ± 5, 35 ± 5, 41 ± 5, and 45 ± 5 eV were used. Thus, TDCS information for momentum transfers ranging from approximately 0.15 to 0.45 a.u. is obtained. Although this binning provided adequate statistics for the binary lobe, generally the statistics for the recoil lobe were marginal. Therefore, broader energy loss bins of $18.3 \pm 2.3, 21.6 \pm 3.3, 25.5 \pm 4.8$, $28.2 \pm 7.6, 33 \pm 7.3, 36 \pm 10$, and 40 ± 10 eV were used.

To convert our measured coincidence yields to TDCS, the detection sensitivity to electrons emitted from an extended volume, rather than from a point, and in the presence of an electric field must be accounted for. In an earlier attempt, we wrote a computer program to model the beam overlap and target region geometry and electric fields to simulate this. However, the results indicated a sharp decrease in detection sensitivity for electrons emitted in the forward and backward directions [27], which led to unphysical increases in the cross sections in both the forward and backward directions. Therefore, for the present study a detailed analysis of SIMION trajectories of electrons emitted from the physical center of the gas jet-beam overlap, plus points 1 and 2 mm up- and downstream as well as 1 and 2 mm above and below the center was performed. Simulations were run for electron energies corresponding to the mean ejected energies of the each of the energy losses listed above. This SIMION investigation yielded much smaller decreases in detection sensitivity than indicated by our previous simulation. As a result, the nonphysical increases in the TDCS in the forward and backward directions were removed. An added benefit was that the present method allowed us to determine which emission angles contributed to the detected signal at each position on our ejected electron channel plate. This was performed for each energy loss bin shown in Fig. 1.

Our measured coincidence yields were converted to relative TDCS by dividing by these SIMION predicted detection efficiencies and adjusting for the different energy loss windows of each binning. These relative TDCS were then placed on an absolute scale by normalizing our electron-impact data to the measurements of Avaldi *et al.* [34] and adjusting these normalized values upward by 13% to account for differences in the total cross sections [32,33] at the slightly different impact energies. (Our normalization to Avaldi *et al.* used the scattering angles and energy losses 3° and 28 ± 2.2 eV for the present paper compared to 3.5° and 26 eV for the Avaldi *et al.* data but slightly different impact energies 250 and 300 eV, respectively.) Finally, after accounting for differences

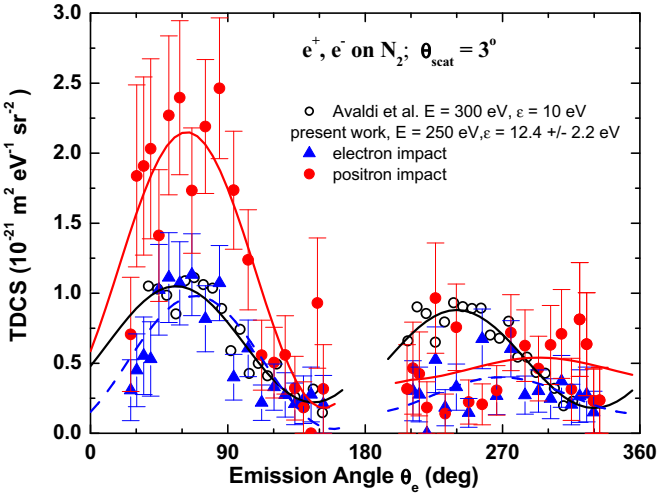

FIG. 5. TDCS data for the ionization of N_2 by 250-eV positrons (filled red circles) and electrons (filled blue triangles) in the present study and for 300-eV electron impact (open black circles) from Avaldi *et al.* [34] as a function of the ejected electrons emission angle (θ_e). In both cases ε is the ejected electron energy. The solid and dashed lines are fits as described in the text.

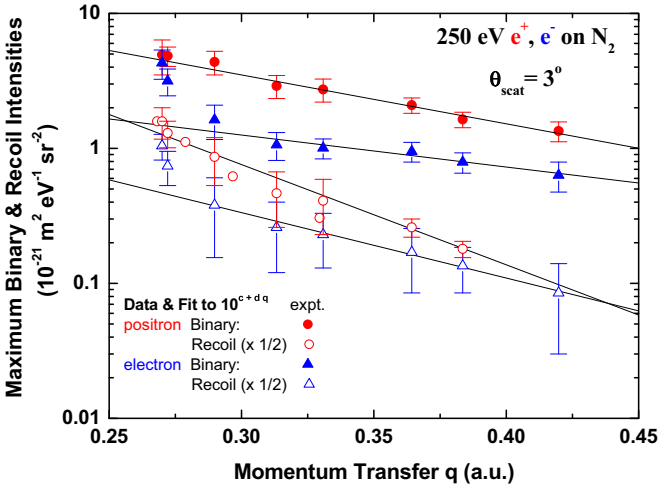

FIG. 6. Maximum intensity of binary (filled symbols) and recoil (open symbols) lobes as a function of momentum transfer q for 250-eV positrons (red circles) and electrons (blue triangles) scattering at 3°. Values are obtained from fitting binned TDCS data. Solid lines are linear fits to the semilogarithmic data. Note that for display purposes the recoil intensities have been divided by 2.

in the total cross sections, this same normalization was used to place the positron data on an absolute scale. However, the reader is cautioned with regard to comparisons on the absolute level since our normalization procedure employed several simplifying assumptions with unknown uncertainties.

Figure 5 shows our normalized positron- and electron-impact TDCS data compared to the electron-impact measurements of Avaldi *et al.* [34] as a function of the angle in which ejected electrons (with known energy) are emitted (emission angle θ_e). To better compare the present results with those of Avaldi *et al.*, the 13% adjustment to account for differences in impact energies has NOT been made, i.e., the absolute cross sections for the present data are 13% larger than values read directly from the figure. Not shown are the uncertainties associated with the range of emission angles, typically $\pm 3°$ to $\pm 4°$, contributing at each point. Also, only statistical error bars are shown for the present data.

The solid and dashed lines are fits to the data that will be described shortly. For binary interactions, the deconvoluted electron-impact data in the present study agree with that reported by Avaldi *et al.* with possible differences in the forward direction. However, the fit to the Avaldi *et al.* data is strongly dependent on a data point at the most forward angle they could measure. Figure 5 clearly shows that positron impact leads to a much more intense binary peak. For the recoil peak the marginal statistics available in the present study make the situation far less clear. Our fitted curves imply nearly identical recoil intensities for positron and electron impact which are considerably smaller than the measurements reported by Avaldi *et al.* This may be entirely due to our very low statistics or may be due to the different impact energies and momenta transfers in making this comparison. Future studies are needed to determine this.

Our binning procedure provides TDCS for many different values of momentum transfer for both positron and electron impact. Therefore, in order to present the information in a compact form as well as to compensate for low statistics in certain cases, simple functions of the form $A + B\cos^2(q_e - q_{max})$ were used to fit the binary and recoil regions. In these functions A represents a background intensity in a $x - y$ plot or the "waist" dimension in a polar plot with $A + B$ being the maximum lobe intensity. θ_e is the electron emission angle, and θ_{max} is the angle of the lobe maximum. As seen in Fig. 5, reasonable fits of the binary and recoil lobes are achieved using this simple function.

These $A + B\cos^2(\theta_e - \theta_{max})$ functions were used to fit all the binned data for the binary and recoil lobes. It was found that fits to the seven broader bins which had better statistics agreed well with fits to the eight smaller bins. Therefore, to minimize the statistical errors, results shown in Figs. 6 and 7 are fits to the first small bin and to the seven broader bins. In addition, to facilitate future comparisons with theory, to extract quantitative differences in the kinematics of positron and electron ionization of N_2 and to provide scaling parameters as a function of the momentum transfer, first-order polynomial fits to the data shown in Figs. 6 and 7 are made with the fitting parameters and their uncertainties listed in Fig. 6 and Table I.

Figure 6 shows the maximum binary (filled symbols) and recoil (open symbols) TDCS intensities ($A + B$) measured for a 3° scattering angle. The units are in units of 10^{-21} m^2 eV^{-1} sr^{-2}. For display purposes, the recoil intensities have been divided by 2. The lines are 10^{c+dq} fits to the data with the fitting parameters c and d listed in Table I. As seen, binary interactions are more probable for positron impact, i.e., when the projectile charge is positive and the Coulomb forces between the projectile and the target electron and with the nucleus are attractive and repulsive, respectively. This is in agreement with theoretical predictions. But, our data imply that for large momentum transfer, the binary lobe intensities will be approximately the same for positron and electron impact. In contrast to theoretical predictions, our

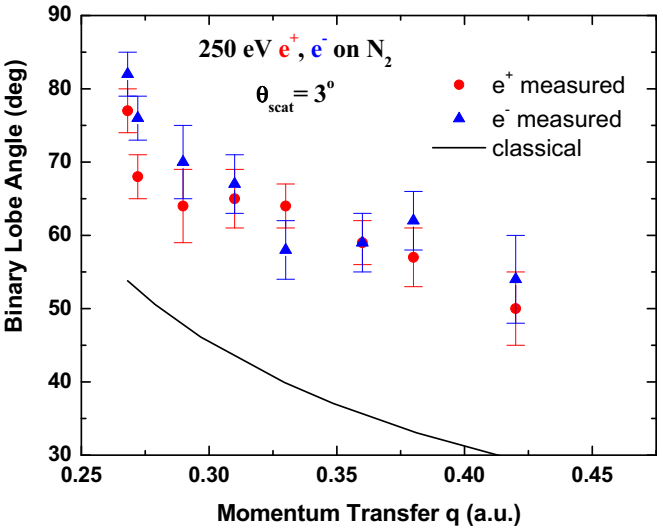

FIG. 7. Direction of the binary lobe for 250-eV positron (filled red circles) and electron (filled blue triangles) impact on molecular nitrogen as a function of momentum transfer. The scattering angle is 3°. The line is the direction obtained from the collision kinematics.

data imply positron impact also leads to a higher probability of recoil interactions. This may be influenced by the low statistics we have for the recoil peak or it could be associated with small momentum-transfer collisions as our fitted curves imply a larger probability for electron impact for higher momentum transfer. Semilogarithmic plots of the binary and recoil intensities are seen to scale linearly with momentum transfer, except for the smallest values of momenta transfer for electron impact. Similar results are found for scattering angles of 1° and 2° where the scaling parameters are listed in Table I. As we believe this increase to be an artifact associated with the large number of very low-energy electrons produced by electron impact, see Fig. 2, the smallest two momenta transfers were not used in fitting the electron-impact data in Fig. 6. However, the recoil or binary lobe intensities were not affected by this increase. The relative magnitudes of the fitting parameters A and B were also investigated and can be determined from values shown in Table II.

Our fitting procedure also provides information about the direction of the binary and recoil lobes. With regard to the binary lobe, a significant portion lies outside our range of sensitivity or where the deconvolution factor is large. This may influence the directions that we obtain when fitting. To test this, we multiplied the convolution factor by $\sin\theta_e$ and found this to: (1) generate unphysical increases in the forward and backward directions, (2) to decrease the direction of the binary lobe even if the unphysical increases at small angles were not included in the fit, but (3) did not strongly influence either the relative difference between the directions obtained for positron and electron impact nor the magnitudes for the binary peak that are shown in Fig. 6. With these factors in mind, Fig. 7 shows the angles where our fit to the binary lobe maximizes. As in the previous figure, the scattering angle is 3°, and the positron- and electron-impact data are shown by filled red circles and blue triangles, respectively. The black line indicates binary lobe directions obtained from the collision kinematics. For scaling predictions, we have fit these data with simple polynomial functions of the momentum transfer with a linear fit being adequate in all but one case. This fitting predicts that the binary lobe maximum (in degrees) is approximately given by $\theta_{\max} = P_1 + P_2 q + P_3 q^2$.

The reader will note that, according to Fig. 6 and the values obtained from Table II, the directions we obtain for both positron and electron impact are significantly larger than those predicted by the collision kinematics whereas for the 600-eV impact ionization of He [2], a slightly larger angle is predicted for electron impact and a slightly smaller angle for positron impact. Future experiments covering a larger angular range and having better statistics will be required to resolve this discrepancy. However the present data do conform with the theoretical predictions that positron impact, i.e., a positive projectile charge, will lead to binary emission that is more forward directed than occurs for a negatively charged projectile.

Figures 6 and 7 and Tables I and III provide information about the trends of the TDCS with respect to momentum transfer, which was one purpose of the fitting procedure. Another purpose was to provide easily accessible cross

TABLE II. Relative magnitude of fitting parameter A for positron and electron impact. Uncertainties are shown by the numbers in brackets.

Scattering angle (deg)		Binary: A/I	Recoil: A/I
1	Electron impact	0.54 (0.13)	0.30 (0.10)
	Positron impact	0.27 (0.03)	0.32 (0.05)
2	Electron impact	0.17 (0.02)	0.42 (0.16)
	Positron impact	0.23 (0.02)	0.29 (0.15)
3	Electron impact	0.18 (0.07)	0.50 (0.17)
	Positron impact	0.08 (0.02)	0.33 (0.13)

TABLE I. Scaling parameters obtained by fitting binary and recoil intensities I for positron and electron impact. The fitting equation used was $I = 10^{c+dq}$ where q is the momentum transfer in atomic units. Uncertainties are shown by the numbers in parentheses. The parameters and uncertainties are in units of 10^{-21} m^2 eV^{-1} sr^{-2}.

Scattering angle (deg)		Binary c	Binary d	Recoil c	Recoil d
1	Electron impact	0.91 (0.16)	–3.14 (0.57)	1.14 (0.07)	–3.90 (0.26)
	Positron impact	1.61 (0.11)	–4.11 (0.40)	1.95 (0.15)	–6.26 (0.53)
2	Electron impact	1.21 (0.11)	–3.77 (0.34)	1.06 (0.11)	–3.69 (0.35)
	Positron impact	1.71 (0.10)	–4.16 (0.31)	2.24 (0.66)	–7.26 (2.48)
3	Electron impact	0.94 (0.16)	–2.71 (0.46)	1.24 (0.08)	–4.74 (0.23)
	Positron impact	1.74 (0.07)	–3.91 (0.21)	2.14 (0.22)	–6.73 (0.65)

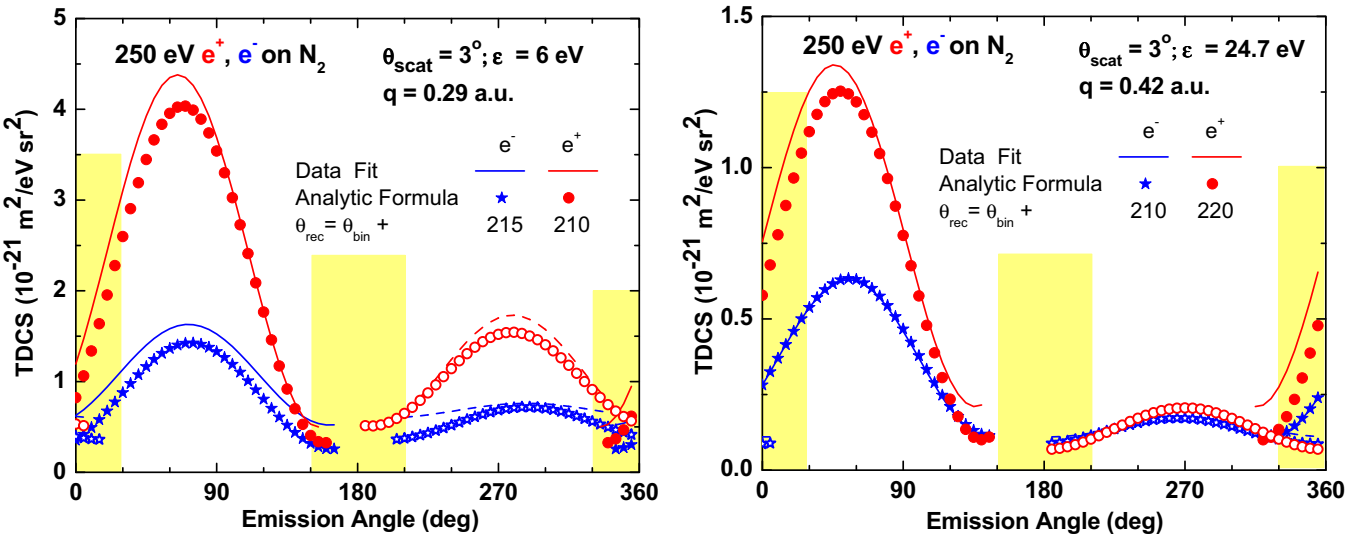

FIG. 8. TDCS obtained using analytic formulas (filled and open symbols) compared to fits to individual data (solid and dashed lines). The yellow rectangles indicate regions outside the viewing range of the ejected electron detector. See the text for details.

sections for comparison to other experimental data or to theoretical predictions. To calculate the TDCS for a particular scattering angle and momentum transfer, values for A, B, and $\theta_{\max}$ are needed for the fitting formula $A + B\cos^2(\theta_e - \theta_{\max})$. A is obtained by multiplying the appropriate fraction in Table II with the corresponding intensity in Table I, and B is 1 minus the same fraction multiplied by the same intensity. $\theta_{\max}$ for the binary lobe is obtained using Table III whereas for recoil interactions it was found that $\theta_{\max}(\text{recoil}) = \theta_{\max}(\text{binary}) + 210$ (for electron impact) and $\theta_{\max}(\text{recoil}) = \theta_{\max}(\text{binary}) + 220$ (for positron impact) yielded good agreement with our individual data fits.

Two examples of cross sections obtained using this procedure are shown by the symbols in Fig. 8. These are compared to actual data fits, shown by the lines. As seen, using the values obtained from our analytical formulas yields agreement within 10% for the range of q values shown. For small q values, which correspond to our lowest ejected electron energies, the analytical formulas for electron impact in Table I underestimate our measured values as was already noted in Fig. 6.

In Fig. 8, the reader is cautioned with respect to the TDCS for recoil interactions and particularly with respect to the direction of the recoil peak because our statistics for recoil interactions, i.e., between 180° and 360° emission angles, are marginal or poor at best. But since little or no TDCS data are available we present findings based upon the available data. For our broader binned fits of the recoil and binary peaks, we obtain an average ratio recoil or binary for all three angles investigated, of 1.31–2.87q for positron impact and a marginally larger value of 1.33–2.58q for electron impact. As before, the momentum transfer q is in atomic units.

TABLE III. Parameters for polynomial fits to binary lobe maximum as a function of momentum transfer, e.g., $\theta_{\max} = p_1 + p_2 q + p_3 q^2$ for 250-eV positron- and electron-impact ionization of N_2. The parameters P_1, P_2, and P_3 (values in the right-hand column with their uncertainties in brackets) are listed.

Scattering angle (deg)		Binary lobe direction (deg) for momentum transfer q in (a.u.)
1	Electron impact	$112(10) - 205(50)q$
	Positron impact	$166(23) - 716(202)q + 815(399)q^2$
2	Electron impact	$101(14) - 145(53)q$
	Positron impact	$128(7) - 255(23)q$
3	Electron impact	$113(11) - 137(54)q$
	Positron impact	$110(8) - 143(25)q$

V. FRAGMENTATION COMPARISONS

As a complementary piece of information and since the experimental device allows us to distinguish both charge state and mass, it was also possible to study the fragmentation

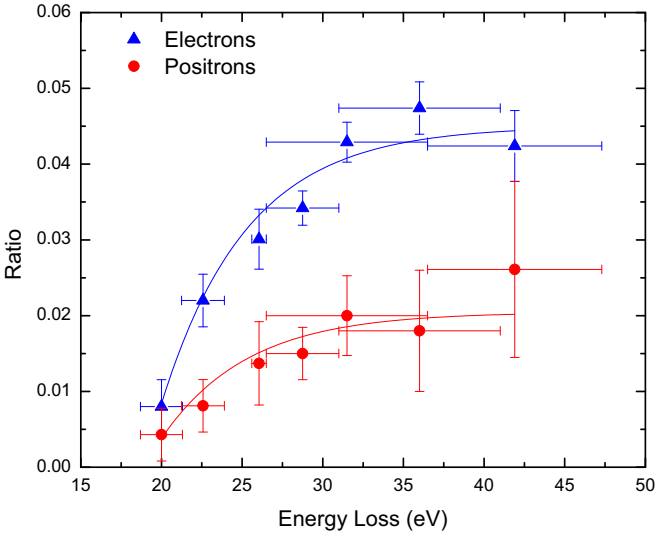

FIG. 9. Ratios of N^+/N_2^+ for electron (black solid squares) and positron (red hollow triangles) impact ionization of N_2. Solid curves are exponential fits of the data.

of N_2 associated with small angle scattering. For this, we considered the number of nitrogen atoms produced with charge state $+1(N^+)$ as well as the number of nitrogen molecules ionized and with charge state $+1(N_2{}^-)$, and then the ratios $N^+/N_2{}^+$ were determined as a function of the energy loss. As seen in Fig. 9, both projectiles exhibit a similar tendency where the fragmentation fraction increases with energy loss. These data indicate that fragmentation of the N_2 molecule is more probable and increases faster for electron impact than for positron impact, whereas ionization without breakup was shown to be more likely for positron impact.

VI. SUMMARY

A detailed comparison of differential ionization of molecular nitrogen has been presented for both positron and electron impact. By comparing experimental data, differences on the singly, doubly, and triply (fully) differential levels that are associated with the sign of the projectile charge were shown. On the doubly differential level, the most notable difference is larger scattering cross sections for positron impact. On the triply differential level, a deconvolution and normalization process was used to place the data on an absolute scale. However, the normalization process employed several assumptions having unknown certainties; therefore the user is cautioned with regard to any comparisons involving absolute magnitudes. An enhancement of binary interactions for positron, as compared to electron, impact was noted, both in the scattered projectile and in the ejected electron channels. This is consistent with theoretical predictions. Theory also predicts that the opposite effect should be observed for the recoil lobe intensities. However, employing the best data analysis we could achieve using the available data we again find larger amplitudes for positron impact; although our data imply that the predicted dominance for electron impact should occur at higher values of momentum transfer. Fits to the binary and recoil amplitudes imply that they scale as a function of momentum transfer. It was shown that TDCS can be easily calculated for any momentum transfer currently investigated using analytic formulas for the fitted values. Information regarding the ionization or fragmentation of the N_2 molecule was also presented and showed higher probabilities that the nitrogen molecule will fragment for electron impact.

ACKNOWLEDGMENTS

Work for the experimental study was supported by the National Science Foundation. The preparation of this paper was supported by UNAM-DGAPA-PAPIIT under Contracts No. TA100213 and No. IN116916.

[1] G. Laricchia, S. Brawley, D. A. Cooke, Á. Kövér, D. J. Murtagh, and A. I. Williams, J. Phys.: Conf. Ser. **194**, 012036 (2009).
[2] S. Sharma and M. K. Srivastava, Phys. Rev. A **38**, 1083 (1988).
[3] M. Brauner, J. S. Briggs, and H. Klar, J. Phys. B: At., Mol. Opt. Phys. **22**, 2265 (1989).
[4] M. Brauner and J. S. Briggs, J. Phys. B: At., Mol. Opt. Phys. **26**, 2451 (1993).
[5] J. Berakdar, J. S. Briggs, and H. Klar, J. Phys. B: At., Mol. Opt. Phys. **26**, 285 (1993).
[6] C. Sinha and S. Tripathit, J. Phys. B: At., Mol. Opt. Phys. **26**, 185 (1993).
[7] R. I. Campeanu, V. Chis, L. Nagy, and A. D. Stauffer, Nucl. Instrum. Methods Phys. Res., Sect. B **221**, 21 (2004).
[8] A. Naja, E. M. Staicu-Casagrande, A. Lahmam-Bennani, M. Nekkab, F. Mezdari, B. Joulakian, O. Chuluunbaatar, and D. H. Madison, J. Phys. B: At., Mol. Opt. Phys. **40**, 3775 (2007).
[9] Á. Benedek and R. I. Campeanu, Nucl. Instrum. Methods Phys. Res., Sect. B **266**, 458 (2008).
[10] O. G. de Lucio, S. Otranto, R. E. Olson, and R. D. DuBois, Phys. Rev. Lett. **104**, 163201 (2010).
[11] G. Purohit, V. Patidar, and K. K. Sud, Nucl. Instrum. Methods Phys. Res., Sect. B **269**, 745 (2011).
[12] R. I. Campeanu and M. Alam, Eur. Phys. J. D **66**, 19 (2012).
[13] R. Dey, A. C. Roy, and C. Dal Cappello, Nucl. Instrum. Methods Phys. Res., Sect. B **271**, 82 (2012).
[14] J. Moxom, G. Laricchia, M. Charlton, G. O. Jones, and Á. Kövér, J. Phys. B: At., Mol. Opt. Phys. **25**, L613 (1992).
[15] A. Schmitt, U. Cerny, H. Möller, W. Raith, and M. Weber, Phys. Rev. A **49**, R5(R) (1994).
[16] Á. Kövér, G. Laricchia, and M. Charlton, J. Phys. B: At., Mol. Opt. Phys. **27**, 2409 (1994).
[17] Á. Kövér, R. M. Finch, M. Charlton, and G. Laricchia, J. Phys. B: At., Mol. Opt. Phys. **30**, L507 (1997).
[18] R. D. DuBois, C. Doudna, C. Lloyd, M. Kahveci, K. Khayyat, Y. Zhou, and D. H. Madison, J. Phys. B: At., Mol. Opt. Phys. **34**, L783 (2001).
[19] A. C. F. Santos, A. Hasan, T. Yates, and R. D. DuBois, Phys. Rev. A **67**, 052708 (2003).
[20] A. C. F. Santos, A. Hasan, and R. D. DuBois, Phys. Rev. A **69**, 032706 (2004).
[21] R. D. DuBois, O. G. de Lucio, and J. Gavin, Europhys. Lett. **89**, 23001 (2010).
[22] Á. Kövér, G. Laricchia, and M. Charlton, J. Phys. B: At., Mol. Opt. Phys. **26**, L575 (1993).
[23] Á. Kövér and G. Laricchia, Phys. Rev. Lett. **80**, 5309 (1998).
[24] Á. Kövér, K. Paludon, and G. Laricchia, J. Phys. B: At., Mol. Opt. Phys. **34**, L219 (2001).
[25] O. G. de Lucio, J. Gavin, and R. D. DuBois, Phys. Rev. Lett. **97**, 243201 (2006).
[26] R. D. DuBois, O. G. de Lucio, and A. C. F. Santos, in *Radiation Physics Research Progress*, edited by A. N. Camilleri (Nova, New York, 2008), p. 105.
[27] R. D. DuBois, J. Phys.: Conf. Ser. **288**, 012011 (2011).
[28] R. D. DuBois, New J. Phys. **14**, 025004 (2012).

[29] J. Gavin, R. D. DuBois, and O. G. de Lucio, J. Phys.: Conf. Ser. **488**, 012058 (2014).
[30] R. D. DuBois, J. Phys.: Conf. Ser. **488**, 012054 (2014).
[31] T. Pflüger, M. Holzwarth, A. Senftleben, X. Ren, A. Dorn, J. Ullrich, L. R. Hargreaves, B. Lohmann, D. S. Slaughter, J. P. Sullivan, J. C. Lower, and S. J. Buckman, J. Phys.: Conf. Ser. **262**, 012047 (2011).
[32] H. Bluhme, N. P. Frandsen, F. M. Jacobsen, H. Knudsen, J. Merrison, K. Paludan, and M. R. Poulsen, J. Phys. B: At., Mol. Opt. Phys. **31**, 4631 (1998).
[33] D. A. Cooke, D. J. Murtagh, and G. Laricchia, Eur. Phys. J. D **68**, 66 (2014).
[34] L. Avaldi, R. Camilloni, E. Fainelli, and G. Stefani, J. Phys. B: At., Mol. Opt. Phys. **25**, 3551 (1992).